IOP Publishing Measurement Science and Technology
Meas. Sci. Technol. 31 (2020) 045102 (16pp) https://doi.org/10.1088/1361-6501/ab5c75

Online blind source separation method with adaptive step size in both time-invariant and time-varying cases

Jiantao Lu, Wei Cheng[1] and Yanyang Zi

State Key Laboratory for Manufacturing Systems Engineering, Xi'an Jiaotong University, Xi'an, 710049, Shaanxi Province, People's Republic of China

E-mail: chengw@xjtu.edu.cn

Received 12 May 2019, revised 6 October 2019
Accepted for publication 27 November 2019
Published 15 January 2020

Abstract

To effectively balance the convergence speed and steady-state error of online blind source separation, this paper develops an online blind source separation method with adaptive step size based on an equivariant adaptive separation via independence (EASI) algorithm. First, we construct a separation indicator from the convergence condition of EASI that can reveal the separation degree of mixed signals. Next, a new forgetting factor suitable for non-stationary cases is designed to reduce the error accumulation of previous data, and the separation indicator can be adaptively updated. To automatically adjust the step size according to separation degree, a nonlinear mapping between the separation indicator and step size is constructed. Finally, numerical and experimental case studies are provided to evaluate the performance of the proposed method, which comparison of results proves to be more effective. The results of numerical case studies show that the step size of the proposed method can be adaptively adjusted in the separation process and the proposed method can effectively balance convergence speed and steady-state error in both time-invariant and time-varying cases. The results of experimental case studies show that the proposed method has higher estimation accuracy.

Keywords: online blind source separation, adaptive step size, equivariant adaptive separation via independence, separation indicator, time-varying case

(Some figures may appear in colour only in the online journal)

1. Introduction

Radiated noises from mechanical systems do not often provide benefits, and therefore it is necessary to identify the sources of these radiated noises [1, 2]. However, this can often be a difficult task in practice since the signals measured by sensors are often a mixture of multiple sources, and thus signal processing is required to obtain pure source information. Furthermore, if a radiated noise source is moving—for example, a navigating underwater vehicle—the measured signals will be time-varying, which is likely to cause some stationary signal processing methods to fail. Therefore, source separation methods are needed in engineering applications not only for time-invariant but also for time-varying cases.

In pioneering research, some methods have been proposed to extract components from measured signals, such as wavelet transform, empirical mode decomposition (EMD), and variational mode decomposition (VMD) [3–5]. Wavelet transforms are based on the inner product transformation principle, which depends largely on the selection of basic functions. EMD is often used to analyze non-stationary data, which are common in many practical situations [6]. However, EMD suffers from a

[1] Author to whom any correspondence should be addressed.

lack of mathematics or interpolation choice, and attracts criticism for being too sensitive to noise and sampling [7, 8]. In addition, EMD is likely to fail given that the signal contains components with some cross-frequency bins. As for VMD, it is an entirely non-recursive variational model from which the modes are extracted concurrently [6]; however, it is still difficult to process signals that contain components with cross-frequency bins.

In the past decades, blind source separation (BSS) has been a prominent issue in the field of signal processing and neural networks [9], and has been widely used in many practical applications [10–14]. In addition, BSS aims to recover statistically independent source signals from mixed signals without any prior knowledge of the source signals or the transmission channel characteristics [15]. Therefore, BSS can almost completely recover source information even for sources with cross-frequency bins. BSS can be roughly classified into two categories: online methods and offline methods [16]. Generally, all data are used in offline methods at each iteration, so that faster convergence rates can be achieved as a result. The well-known fixed-point algorithm [17] usually obtains satisfactory results after a few iterations in separation procedures. However, one unsatisfactory aspect of offline BSS methods is that they need large storage capacity and so are not suitable for time-varying cases. In contrast, online methods only need a small amount of data storage and deal with newly updating data in real time. Some classical online BSS methods have often been applied to practice, such as the natural gradient algorithm [18], the equivariant adaptive separation via independence (EASI) algorithm [19] and the iterative inversion independent component analysis (ICA) algorithm [20]. In fact, online BBS methods can dynamically update the unmixing matrix with current data, and therefore they have been successfully used in time-varying cases.

There are many important indicators for evaluating the performance of online BSS methods, among which the parameters of convergence rate and steady-state error are frequently used and observed. Step size is a key parameter that significantly influences convergence performance [21]. Generally, a faster convergence rate is required to quickly track the changes of the system, and a smaller steady-state error is also necessary to accurately recover source signals for satisfactory results. However, traditional online BSS methods usually cannot effectively balance the convergence rate and the steady-state error due to the limitation of fixed step size [22]. An alternative approach is to adjust the step size according to the exponential decay form [23], and in this way, better results can be obtained as anticipated. However, when the source signals have not been well recovered and the step size has been reduced to a small value, the convergence rate can become very slow accordingly. To address such problems, Zhang *et al* suggested adjusting the step size in accordance with the correlation coefficients of the separated signals [24], which can reveal the separation degree of mixed signals. At different stages, different step sizes are used for each output component. However, this method is relatively complex and unsuitable for signals with high sampling frequency. Based on the orthogonal constraint of the separating matrix, Tang *et al* proposed an adaptive-step-size natural-gradient ICA method [25] that regards the convergence condition as the controller of the step size; however, Tang's method did not combine the convergence condition of the natural gradient with the orthogonal constraint to adjust the step size. As a result, the effectiveness of this method could not be as well ensured as suggested. Xu *et al* introduced a variable-step-size method based on a reference separation system [26], with the step size controlled by the mean square error between the main separation system and the reference separation system. However, the results are still not satisfactory when the mixing matrix is time-varying.

Summarizing the achievements of previous studies and current shortages in the field of signal processing, this paper introduces an online blind source separation method with adaptive step size based on an EASI algorithm in an attempt to address problems in both time-invariant and time-varying cases. First, to reveal the separation degree of mixed signals, an effective separation indicator (SI) is constructed with the convergence condition of the EASI algorithm. Second, recursive updating equations of the SI are derived using a forgetting factor that can reduce the error accumulation of previous data. The SI can then be adaptively updated during the separation process. Third, a sigmoid function is adopted to adjust the step size according to the SI, and therefore the step size can be also adjusted according to the separation degree of mixed signals. Some numerical and experimental studies are carried out to verify the effectiveness of the proposed method. According to the results, the proposed method tends to perform better than the contrast methods in both time-invariant and time-varying cases.

The organization of this paper is as follows: In section 2, the basic theory of the online BSS method is briefly introduced. In section 3, the proposed adaptive-step-size online BSS method is given. In section 4, some numerical case studies are provided to assess the effectiveness of the proposed method. In section 5, a test bed is built and BSS algorithms are comparatively studied with real acoustic signals. In section 6, conclusions of this study are drawn.

2. Online BSS methods

2.1. System model

Assume that $s_k = [s_{1k}, s_{2k}, \cdots, s_{mk}]^T$ and $x_k = [x_{1k}, x_{2k}, \cdots, x_{mk}]^T$ are the source signal vector and the mixed signal vector, respectively, where $k = 1, 2, \cdots, K$ represents the discrete time; m is the source number, and the number of mixed signals is also assumed to be m; and $[\cdot]^T$ denotes the matrix transpose operator. The linear instantaneous mixing model of the online BSS method is typically formulated as

$$x_k = \mathbf{A}s_k \tag{1}$$

where $\mathbf{A}$ is the full-rank $m \times m$ mixing matrix. Generally, source signals are assumed to be statistically independent, and without any loss of generality, they are also assumed to have zero means, unit variances and at most one of them has a Gaussian distribution. The ultimate objective of the online

BSS method is to recover unknown sources from their mixtures, i.e. to find an optimal separating matrix $\mathbf{W}$ that yields the following function:

$$y_k = \mathbf{W}x_k \tag{2}$$

where $y_k = [y_{1k}, y_{2k}, \cdots, y_{mk}]^T$ represents the separated signal vector. If $\mathbf{A}$ is an invertible matrix and $\mathbf{W} = \mathbf{A}^{-1}$, then $y_k = \mathbf{W}x_k = \mathbf{A}^{-1}\mathbf{A}s_k = s_k$ is an estimation of a source signal vector. The objective of the online BSS method is to obtain the estimated source signals y_k by optimizing the separating matrix.

2.2. Typical online BSS algorithms

In BSS, the independence of separated signals is often used as the objective function to update the separating matrix. Mutual information is an effective tool to evaluate the interdependence degree between separated signals. Based on mutual information, the natural-gradient method [18] can be used to update the separating matrix by

$$\mathbf{W}(k+1) = \mathbf{W}(k) + \mu\left[\mathbf{I} - \Phi(y_k)\, y_k^T\right]\mathbf{W}(k) \tag{3}$$

where $\mathbf{W}(k)$ is the kth iteration of the separating matrix; μ is the step size; $\mathbf{I}$ is a unit matrix; $\Phi(\cdot) = [\phi_1(\cdot), \cdots, \phi_n(\cdot)]^T$ is the score function; and $\phi_k(\cdot)$ is an odd nonlinear function that acts upon the elements of y_k. The choice of score function depends on the probability distributions of source signals. The pre-whitening of mixed signals is necessary to make separation simpler and more effective, thus making the separated signals uncorrelated as well. Similar to equation (3), the pre-whitening of mixed signals can be achieved by updating the separating matrix with

$$\mathbf{W}(k+1) = \mathbf{W}(k) + \mu\left(\mathbf{I} - y_k y_k^T\right)\mathbf{W}(k). \tag{4}$$

Combining equations (3) and (4), the EASI algorithm [27–29] can be expressed as

$$\mathbf{W}(k+1) = \mathbf{W}(k) + \mu\left[\mathbf{I} - y_k y_k^T + y_k\Phi^T(y_k) - \Phi(y_k)\, y_k^T\right]\mathbf{W}(k). \tag{5}$$

3. Proposed online BSS method with adaptive step size

3.1. Separation indicator

As mentioned previously, step size is an important parameter that influences the convergence performance of online BSS methods. Obviously, step size should be adjusted according to the separation degree of mixed signals. Therefore, the SI is constructed first from the convergence condition of EASI, and can reveal the separation degree of mixed signals.

According to equation (5), when the convergence condition of EASI is reached, we can obtain

$$E\left[\mathbf{I} - y_k y_k^T + y_k\Phi^T(y_k) - \Phi(y_k)\, y_k^T\right] = \mathbf{0} \tag{6}$$

where $E[\cdot]$ represents mathematical expectation and $\mathbf{0}$ is a zero matrix. Let

$$\mathbf{B}_1 = E\left[\mathbf{I} - y_k y_k^T\right] \quad \text{and} \quad \mathbf{B}_2 = E\left[y_k\Phi^T(y_k) - \Phi(y_k)\, y_k^T\right]. \tag{7}$$

From equation (7), we have $\mathbf{B}_1^T = \mathbf{B}_1$ and $\mathbf{B}_2^T = -\mathbf{B}_2$, that is, $\mathbf{B}_1$ and $\mathbf{B}_2$ are a symmetric matrix and a skew symmetric matrix, respectively. It is worth noting that the diagonal elements of $\mathbf{B}_2$ equal zero. Then, $\mathbf{B}_1$ and $\mathbf{B}_2$ can be rewritten as

$$\mathbf{B}_1 = \begin{bmatrix} b_{11}^1 & b_{12}^1 & \cdots & b_{1N}^1 \\ b_{12}^1 & b_{22}^1 & \cdots & b_{2N}^1 \\ \vdots & \vdots & \ddots & \vdots \\ b_{1N}^1 & b_{2N}^1 & \cdots & b_{NN}^1 \end{bmatrix} \quad \text{and} \quad \mathbf{B}_2 = \begin{bmatrix} 0 & b_{12}^2 & \cdots & b_{1N}^2 \\ -b_{12}^2 & 0 & \cdots & b_{2N}^2 \\ \vdots & \vdots & \ddots & \vdots \\ -b_{1N}^2 & -b_{2N}^2 & \cdots & 0 \end{bmatrix} \tag{8}$$

where b_{mn}^l represents the (m, n) element of $\mathbf{B}_l$. Combining equations (7) and (8) with (6), we obtain

$$b_{ii}^1 = 0 \quad i = 1, 2, \cdots, N \tag{9}$$

$$\begin{cases} b_{ij}^1 + b_{ij}^2 = 0 \\ b_{ij}^1 - b_{ij}^2 = 0 \end{cases} \Rightarrow \begin{cases} b_{ij}^1 = 0 \\ b_{ij}^2 = 0 \end{cases} \quad i, j = 1, 2, \cdots, N \text{ and } i \neq j. \tag{10}$$

Thus, equations (9) and (10) can be expressed in matrix form as

$$\mathbf{B}_1 = \mathbf{0} \quad \text{and} \quad \mathbf{B}_2 = \mathbf{0}. \tag{11}$$

Therefore, when the method comes to the convergence conditions, we can obtain

$$\|\mathbf{B}_1\| = 0 \quad \text{and} \quad \|\mathbf{B}_2\| = 0 \tag{12}$$

where $\|\cdot\|$ represents a matrix norm that can be 1-norm, 2-norm or ∞-norm. Thus, the SI can be defined as

$$\zeta = \max\left(\|\mathbf{B}_1\|, \|\mathbf{B}_2\|\right) \tag{13}$$

where $\max(\cdot)$ represents the maximum of elements in the bracket.

According to equation (13), ζ is nonnegative, and $\zeta = 0$ if and only if equation (12) holds. At the initial stage, the separation degree of mixed signals is low and ζ will be large. As the separation process goes on, the separated signals are increasingly similar to the source signals, i.e. the separation degree of mixed signals is increasing. At this time, ζ will become extremely small because equation (12) is nearly satisfied when the EASI algorithm approaches the anticipated convergence degree. As a result, ζ will gradually decrease during the separation process, and therefore can reveal the separation degree of mixed signals.

3.2. Online updating of separation indicator

In online BSS methods, parameters should be updated recursively to reduce the computational complexity at each iteration. From equation (13), to obtain ζ, $\mathbf{B}_1$ and $\mathbf{B}_2$ should be adaptively updated. Let

$$\begin{cases} \mathbf{R}_L = E\left[y_k y_k^T\right] \\ \mathbf{R}_H = E\left[\Phi(y_k)\, y_k^T\right] \end{cases}, \quad k = 1, 2, \cdots, K. \tag{14}$$

To obtain $\mathbf{B}_1$ and $\mathbf{B}_2$, the adaptive updates of $\mathbf{R}_L$ and $\mathbf{R}_H$ need to be acquired in advance. The separated signals at the

initial stage are largely different from the source signals. As the separation process goes on, the separation error will be gradually reduced to a small value. Therefore, a forgetting factor [24, 30] is usually used to reduce error accumulation at the initial stage. The mean of a stationary discrete signal h_t $t = 1,\ 2,\ \cdots$, can be updated [24] using a forgetting factor according to

$$\begin{aligned}\bar{h}(k) &= \eta\bar{h}(k-1)/k + h_k/k \\ &= \left(h_k + \eta h_{k-1} + \cdots + \eta^{k-1}h_1\right)/k\end{aligned} \tag{15}$$

where $0 < \eta < 1$ is the forgetting factor. In equation (15), h_t must be a stationary signal; however, the elements of $\mathbf{R}_{\mathrm{L}}$ and $\mathbf{R}_{\mathrm{H}}$ often vary a lot during the separation process. Therefore, it is not suitable to update $\mathbf{R}_{\mathrm{L}}$ and $\mathbf{R}_{\mathrm{H}}$ using equation (15).

The method used in this study is that, after being updated, the previous data are weighted by η and the total number of previous data is also weighted by η, that is, $\bar{\mathbf{R}}_{\mathrm{L}}$ and $\bar{\mathbf{R}}_{\mathrm{H}}$ are adaptively updated by

$$\begin{cases}\bar{\mathbf{R}}_L(k) = \left[y_k y_k^T + \eta\Gamma_\eta(k-1)\,\bar{\mathbf{R}}_L(k-1)\right]/\Gamma_\eta(k) \\ \bar{\mathbf{R}}_H(k) = \left[\Phi(y_k)\,y_k^T + \eta\Gamma_\eta(k-1)\,\bar{\mathbf{R}}_H(k-1)\right]/\Gamma_\eta(k)\end{cases} \tag{16}$$

where $\Gamma_\eta(k)$ represents the kth total number and $\Gamma_\eta(k) = 1 + \eta + \cdots + \eta^{k-1}$. $\Gamma_\eta(k)$ can be adaptively updated by

$$\Gamma_\eta(k) = 1 + \eta\Gamma_\eta(k-1). \tag{17}$$

The smooth method [25] is adopted considering the effect of the previous step by

$$\begin{cases}\mathbf{R}_L(k) = [1-\mu(k-1)]\,\mathbf{R}_L(k-1) + \mu(k-1)\,\bar{\mathbf{R}}_L(k-1) \\ \mathbf{R}_H(k) = [1-\mu(k-1)]\,\mathbf{R}_H(k-1) + \mu(k-1)\,\bar{\mathbf{R}}_H(k-1)\end{cases}. \tag{18}$$

From equation (7), $\mathbf{B}_1$ and $\mathbf{B}_2$ can be updated to

$$\begin{cases}\mathbf{B}_1(k) = \mathbf{I} - \mathbf{R}_L(k) \\ \mathbf{B}_2(k) = \mathbf{R}_{\mathrm{H}}^{\mathrm{T}}(k) - \mathbf{R}_{\mathrm{H}}(k)\end{cases}. \tag{19}$$

3.3. Adaptive update of the step size

The step size is important in controlling the updating magnitudes of the separating matrix [25, 29]. Therefore, an appropriate step size has a great effect on the separation performances of online BSS methods. When the step size is large, a fast convergence rate can be obtained as a result, but it may lead to a large steady-state error. Too large a step size can even give rise to the possibility that online BSS algorithms do not converge as expected. However, if the step size is too small, the slow convergence rates will lead to poor tracking performance. Therefore, the step size should be adaptively adjusted with the SI ζ to obtain a faster convergence rate and a smaller steady-state error simultaneously. In this study, a nonlinear mapping is presented to dynamically adjust the step size according to ζ.

Since the separated signals are significantly different from the source signals at the initial stage, it is reasonable to choose a larger step size to speed up the separation process. As the separation goes on, the step size should be gradually decreased with ζ. Therefore, to describe the trend of the step size, the hyperbolic tangent function is adopted as

$$\bar{\mu}(k) = \beta\tanh\{\alpha[\zeta(k) - \delta]\} + \gamma \tag{20}$$

where α represents the shape factor and β is the scale factor. Their effects on the performance of the proposed method will be investigated in section 4.1. δ represents the position with maximum variance rate of ζ. Satisfactory results can be obtained when δ is equal to about half of the maximum ζ; γ is used to ensure that $\bar{\mu}(k) = 0$ for $\zeta(k) = 0$. Therefore, from equation (20), we can get

$$\gamma = -\beta\tanh(-\alpha\cdot\delta). \tag{21}$$

Since the current step size is also affected by the previous step size [31], μ is adaptively updated by

$$\mu(k) = \upsilon\mu(k-1) + (1-\upsilon)\,\bar{\mu}(k). \tag{22}$$

The framework of the proposed online BSS method with adaptive step size is shown in figure 1.

4. Numerical case study

4.1. Parameter selection

To illustrate the effectiveness of the proposed forgetting factor method in section 3.2, a mean tracking case is studied in this research. A segmented function $f(t)$ is used as the original signal, the mean of which needs to be tracked, and is in the form of $f(t) = \{5e^{-10t},\ t\in[0,1];\ 3e^{-5(t-2)},\ t\in[2,3];5e^{-10(t-4)},\ t\in[4,\ 5];\ 0,\ \text{Otherwise}\}$. The sampling frequency is 5000 Hz. Gauss white noise is added to $f(t)$ and the signal-to-noise ratio (SNR) is 20 dB.

Figure 2 shows the comparison of the tracking speed and the tracking error of the proposed forgetting factor method with the conventional forgetting factor method when $\eta = 0.98$. As shown in figure 2(a), the tracking speed of the proposed method is much faster than that of the conventional method at the initial stage. Moreover, the proposed method can quickly track $f(t)$ when it abruptly changes. From figure 2(b), the error of the proposed method is a little larger only at the initial stage and when $f(t)$ abruptly changes, but the error is quickly reduced to a small value. The error of the conventional method is larger than that of the proposed method, which illustrates the effectiveness of the proposed forgetting factor method in non-stationary cases.

To show the influence of α and β on the performance of the proposed method, the following numerical studies are conducted using six source signals and six mixtures of them. The source signals are $s = \{s_{1t};\ s_{2t};\ s_{3t};\ s_{4t};\ s_{5t};\ s_{6t};\} = \{sin[\cos(310\pi t)];, \sin(1600\pi t);\ \sin(18\pi t);\ \sin[600\pi t + 6\cos(120\pi t)];\sin(18\pi t)\sin(600\pi t);\ r\ \text{and}\ n(-1, 1)$, which are a square-wave signal, high-frequency sinusoidal signal, low-frequency sinusoidal signal, phase-modulation signal, amplitude-modulation signal, and white-noise signal, respectively. The sampling frequency and sampling length are set as 10 000 Hz and 1 s, respectively. In the experiments, 100 Monte Carlo trials are carried out to evaluate the average convergence performances of the proposed method. s_{6t} is

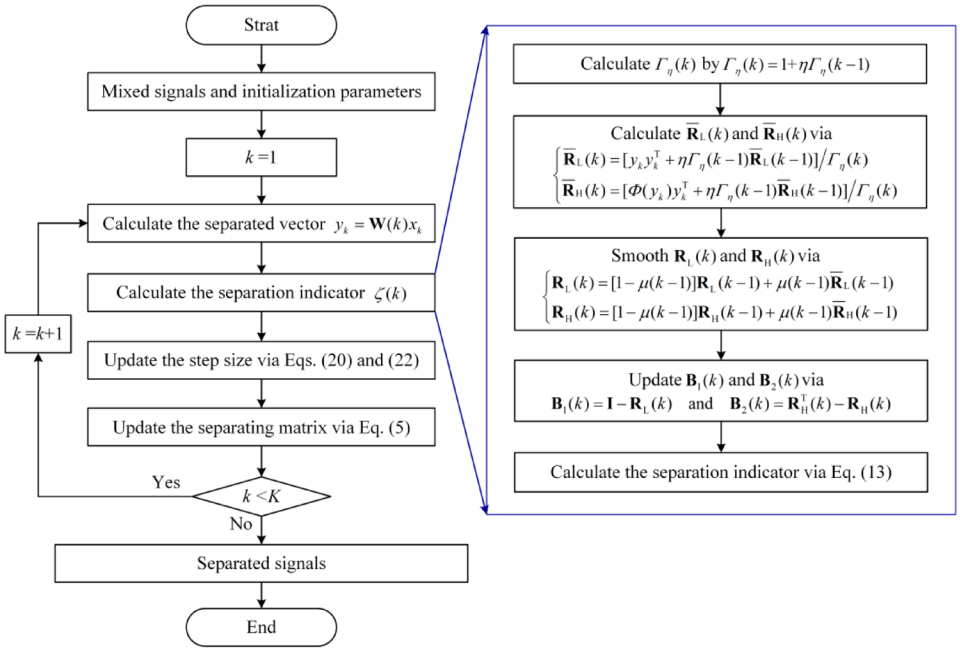

Figure 1. Framework of the proposed online BSS method with adaptive step size.

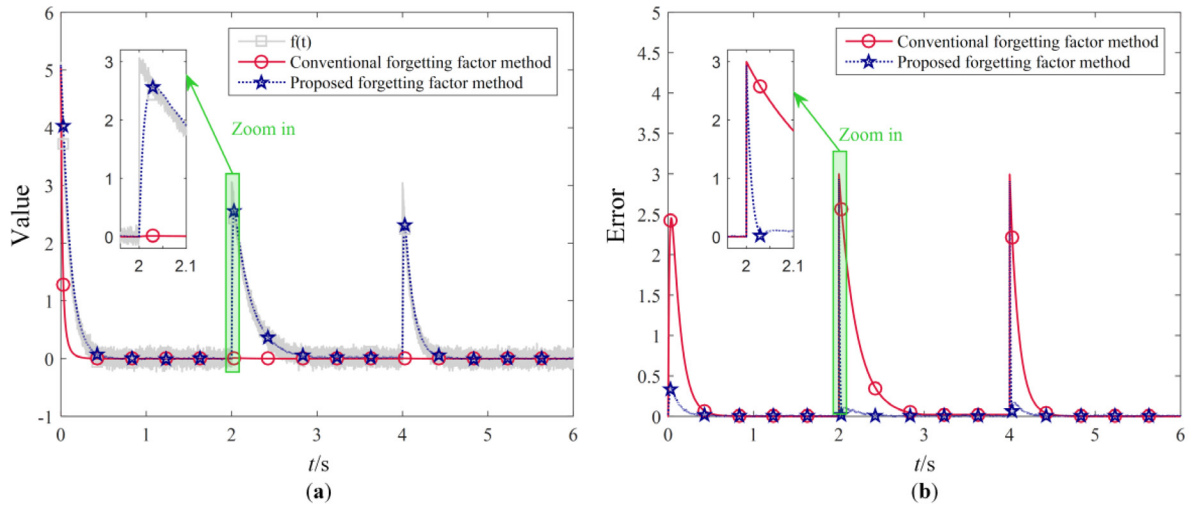

Figure 2. Tracking performance comparison between the conventional forgetting factor method and the proposed forgetting factor method. (a) Tracking speed; (b) tracking error.

randomly generated for each trial. Furthermore, the mixing matrix $\mathbf{A}$, also randomly generated for each trial, is subject to normal distribution $N(0,1)$ .The average performance index (API) of 100 Monte Carlo trials [25], as a function of the global matrix $\mathbf{C} = \mathbf{WA}$, is mainly used to test performances of the proposed method:

$$\mathrm{PI} = \sum_i \left(\sum_j \frac{|\mathbf{C}_{ij}|}{\max_k |\mathbf{C}_{ik}|} - 1 \right) + \sum_j \left(\sum_i \frac{|\mathbf{C}_{ij}|}{\max_k |\mathbf{C}_{kj}|} - 1 \right) \tag{23}$$

where $\mathbf{C}_{ij}$ is the $(i,\ j)$ element of the global matrix $\mathbf{C}$. The performance index (PI) ideally attains its minimum value, zero, when the separation is achieved.

In this numerical study, $\phi(x) = x^3$ is used as the score function and δ is set as 0.7. Figure 3 reveals the convergence performances with different α and β. As shown in figure 3(a), α has a great effect on the steady-state error, which decreases as α decreases. From figure 3(b), the initial convergence rate is mainly affected by β, mainly because β controls the initial step size. The larger β is, the larger the initial step size will be, leading to a larger initial convergence rate. In the following part of this study, α and β are set as 4 and 0.005, respectively.

4.2. Numerical case studies in time-invariant cases

4.2.1. Harmonic signals. To show the effectiveness and stability of the proposed method, the following numerical studies are performed in time-invariant cases. Four typical signals $s = \{s_{1t};\ s_{2t};\ s_{3t};\ s_{4t}\} = \{\sin(1600\pi t);\ \sin(180\pi t);\ \sin(18\pi t)\sin(600\pi t);\ 1 - 2rand(1, 10\,000)\}$ are used as source signals. Source signal s_{4t} is used to simulate environmental noise, and Gauss white noise with a different

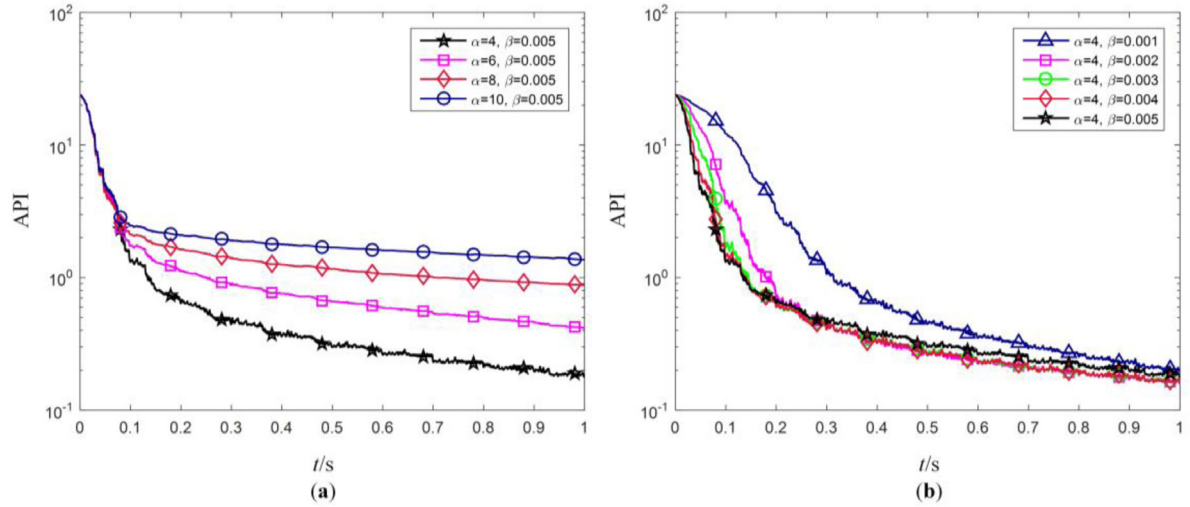

Figure 3. Convergence performances with different parameters. (a) Different α; (b) different β.

SNR is added to the mixed signals to simulate the measured noise. The proposed method is compared with two fixed-step-size methods, i.e. the natural-gradient method with fixed step size (FS-NG) and the EASI method with fixed step size (FS-EASI), and two variable-step-size methods, i.e. the exponential-decay-step-size method (EDS) [23] and the adaptive-step-size method with weighted orthogonalization (AS-WO) [25]. The sampling frequency and the sampling length are 10 000 Hz and 1 s, respectively.

Besides API, the SNR [32] of the separated signals is also used to evaluate the performances of these methods, and is defined as

$$\mathrm{SNR} = 10\log_{10}\left(\sigma^2/\mathrm{MSE}\right) \tag{24}$$

where σ^2 denotes the variances of the source signals and MSE denotes the mean square errors between the source signals and separated signals. Because of the scale indeterminacy of the BSS method, it is necessary to normalize the separated signals and source signals while calculating σ^2 and MSE. When the separated signals are similar to the source signals, MSE tends to become small accordingly in the ongoing process. Hence, the performance of the method is better if it has greater SNR.

The initial parameters are set as follows: the step sizes of both FS-NG and FS-EASI are set as $\mu = 0.01$; and the parameters of EDS are set as $\mu_0 = 1.4 \times 10^{-2}$, $K_0 = 5 \times 10^2$, and $K_d = 1.5 \times 10^{-3}$, which are widely used in [24, 25]. In AS-WO, the error matrix is in the form of

$$\mathbf{H}_2 = \mathbf{I} - \mathbf{B}\mathbf{R}_\mathbf{X}\mathbf{B}^T \tag{25}$$

where $\mathbf{H}_2$ is the error matrix, $\mathbf{I}$ is the identity matrix, $\mathbf{B}$ is the separating matrix and $\mathbf{R}_\mathbf{X}$ is the correlation matrix of mixed signals. The reason why we chose $\mathbf{H}_2$ is that the results obtained using $\mathbf{H}_2$ are better than when using $\mathbf{H}_1(k) = \mathbf{I} - \Phi(y_k)\, y_k^T$ (the other error matrix in [25]). Other parameters in AS-WO are set as $\mu_0 = 1 \times 10^{-2}$, $\beta = 0.998$, and $\rho = 0.002$. In the proposed method, $\alpha = 4$, $\beta = 0.005$, $\delta = 0.7$, $\eta = 0.98$, and the norm form in equation (13) is the 1-norm.

Source signals and mixed signals of a separation example with SNR = 20 dB are presented in figures 4(a) and (b), respectively. The separated signals recovered by the proposed method are shown in figure 4(c) and their order has been adjusted according to the source signals. Comparing figures 4(c) and (a), we find that the source signals have been well recovered, indicating the effectiveness of the proposed method.

Figure 5 shows the performance comparison of the different methods. Figure 5(a) shows the API obtained from FS-NG, FS-EASI, EDS, AS-WO, and the proposed method. From figure 5(a), the convergence speed of FS-EASI is faster than that of FS-NG because of the use of the orthogonal constraint of the separating matrix in FS-EASI. However, the steady-state errors of FS-NG and FS-EASI are relatively large and have large fluctuation due to the limitation of fixed step size. The proposed method has smaller steady-state error compared with FS-NG and FS-EASI. Compared with EDS and AS-WO, the proposed method has faster convergence speed and smaller steady-state error. Figure 5(b) shows the standard deviation (STD) of the PI of the 100 Monte Carlo trials. As revealed in figure 5(b), although the STD of the proposed method is slightly larger than that of FS-EASI at the initial stage, it reaches the minimum value after only 0.1 s, indicating that the proposed method has better numerical robustness. The above results show that the proposed method can perform better than the contrast methods. It should be noted that the convergence speed in this paper is not presented by the computational time but by the sample points. The method has faster convergence speed, which means that it requires fewer sampling points for the PI to reach the same value.

Figure 6 shows the variations of the average SI and average step size of the proposed method, and reveals that the variation of both the SI and the step size can be divided into three stages: (I) Initial stage. The SI increases from zero to the maximum, so the step size increases rapidly to accelerate the convergence; (II) Estimation stage. The separated signals are increasingly similar to the source signals, so the SI decreases quickly, and therefore the step size decreases as the SI decreases; (III) Stabilization stage. The separated signals have been well recovered, so the SI and the step size remain at

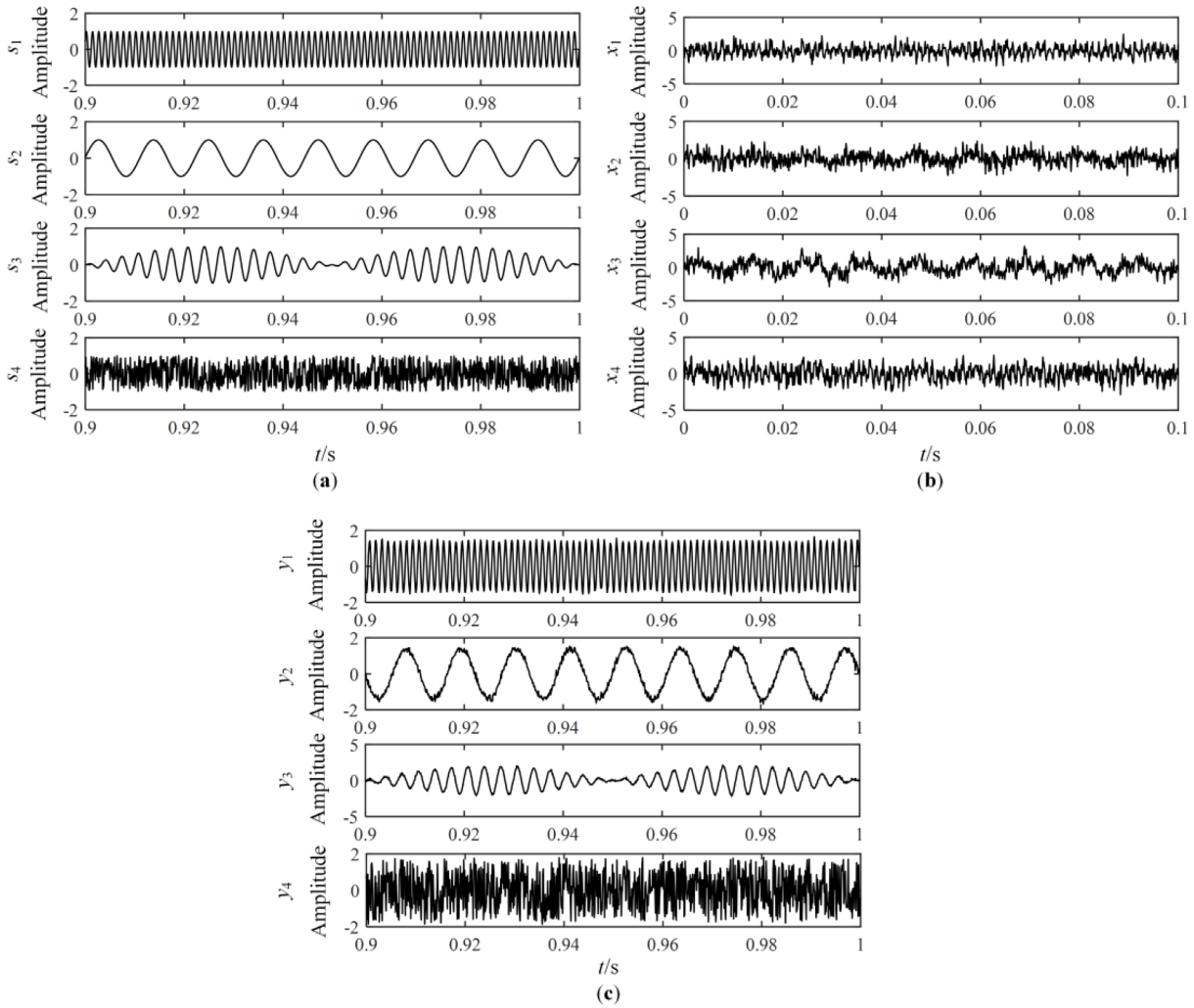

Figure 4. Separation example of the proposed method using harmonic signals in a time-invariant case. (a) Source signals; (b) mixed signals; (c) separated signals.

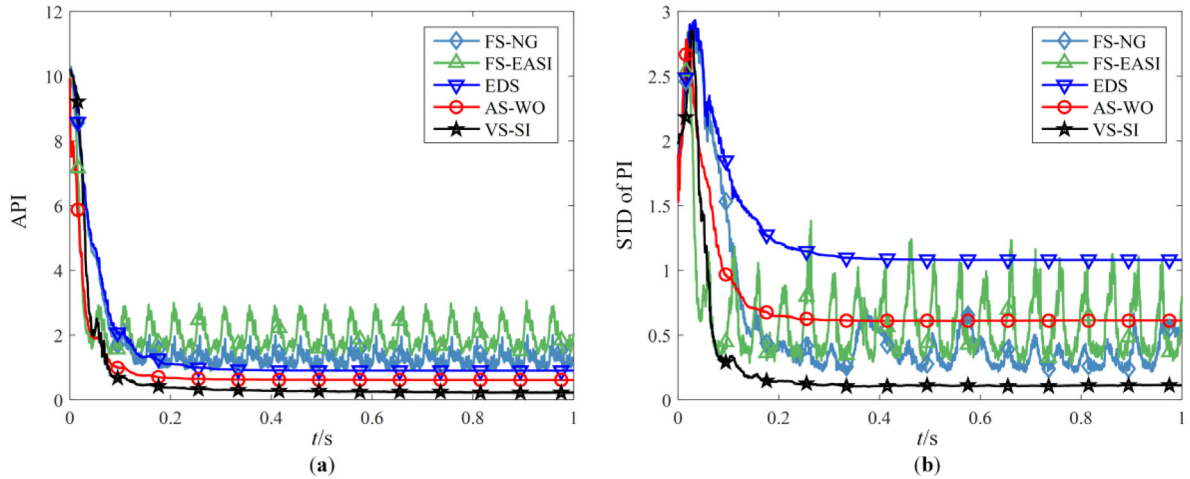

Figure 5. Performance comparison using harmonic signals in time-invariant cases. (a) API; (b) STD of PI.

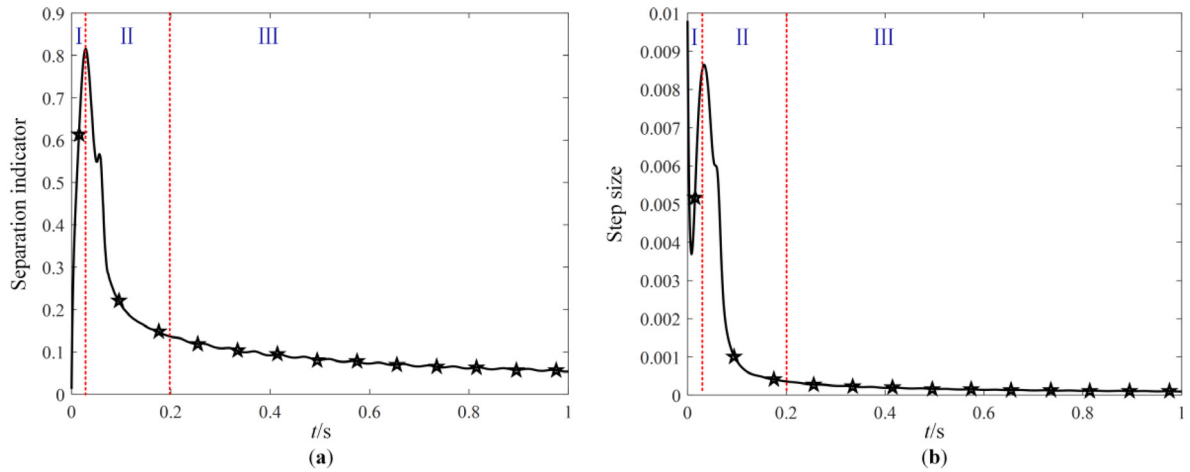

Figure 6. Variation of the SI and the step size of the proposed method in time-invariant cases. (a) SI; (b) step size.

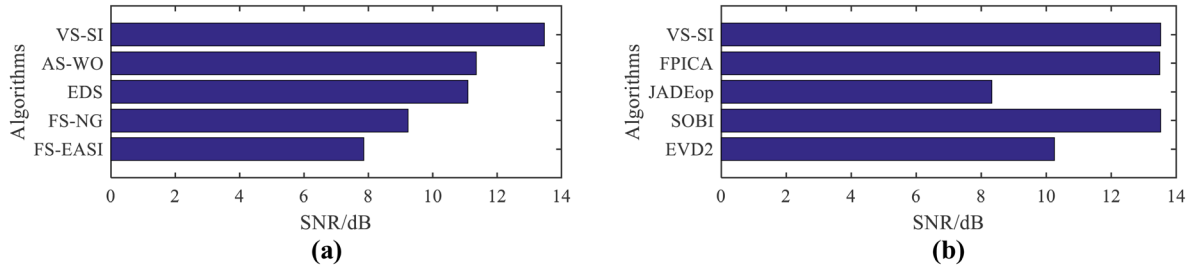

Figure 7. SNR comparison using harmonic signals in time-invariant cases. (a) Comparison with online methods; (b) comparison with offline methods.

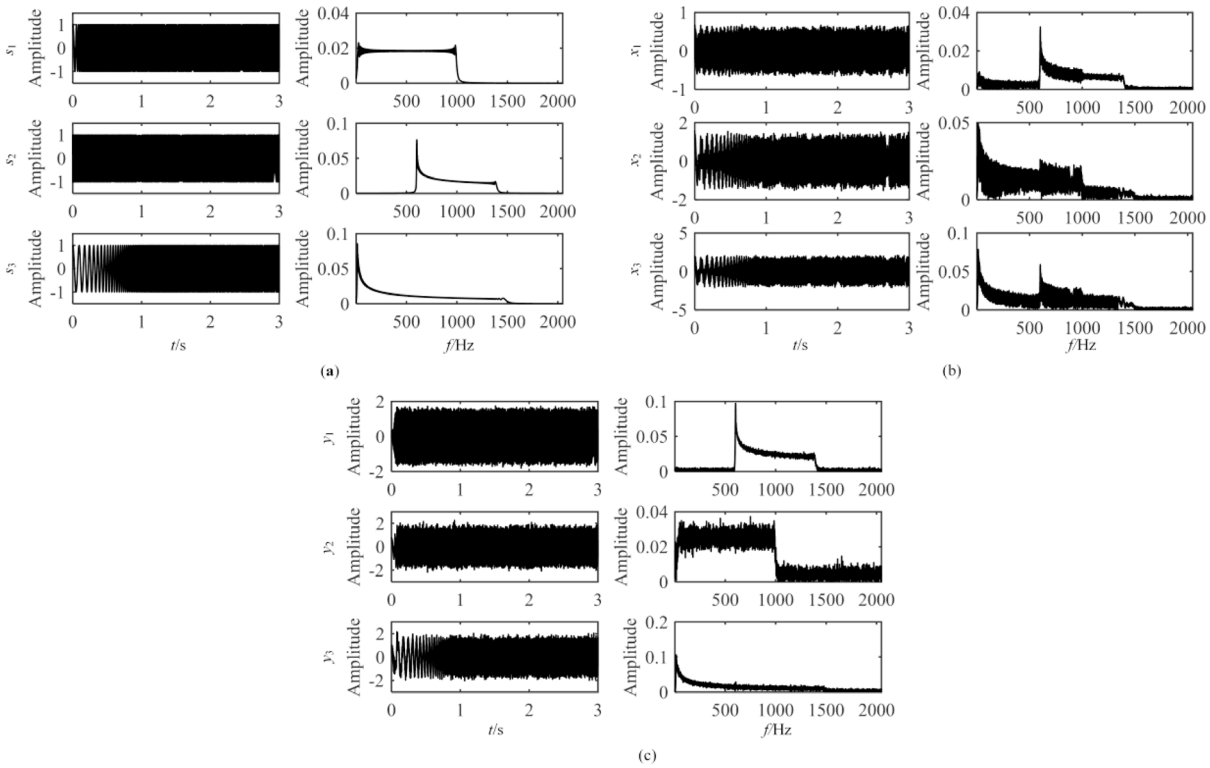

Figure 8. Separation example of the proposed method using wide-band signals in time-invariant cases. (a) Source signals; (b) mixed signals; (c) separated signals.

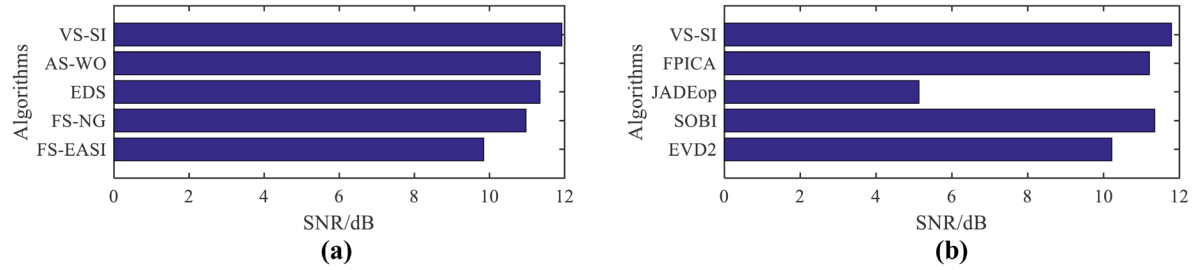

Figure 9. SNR comparison using wide-band signals. (a) Comparison with online methods; (b) comparison with offline methods.

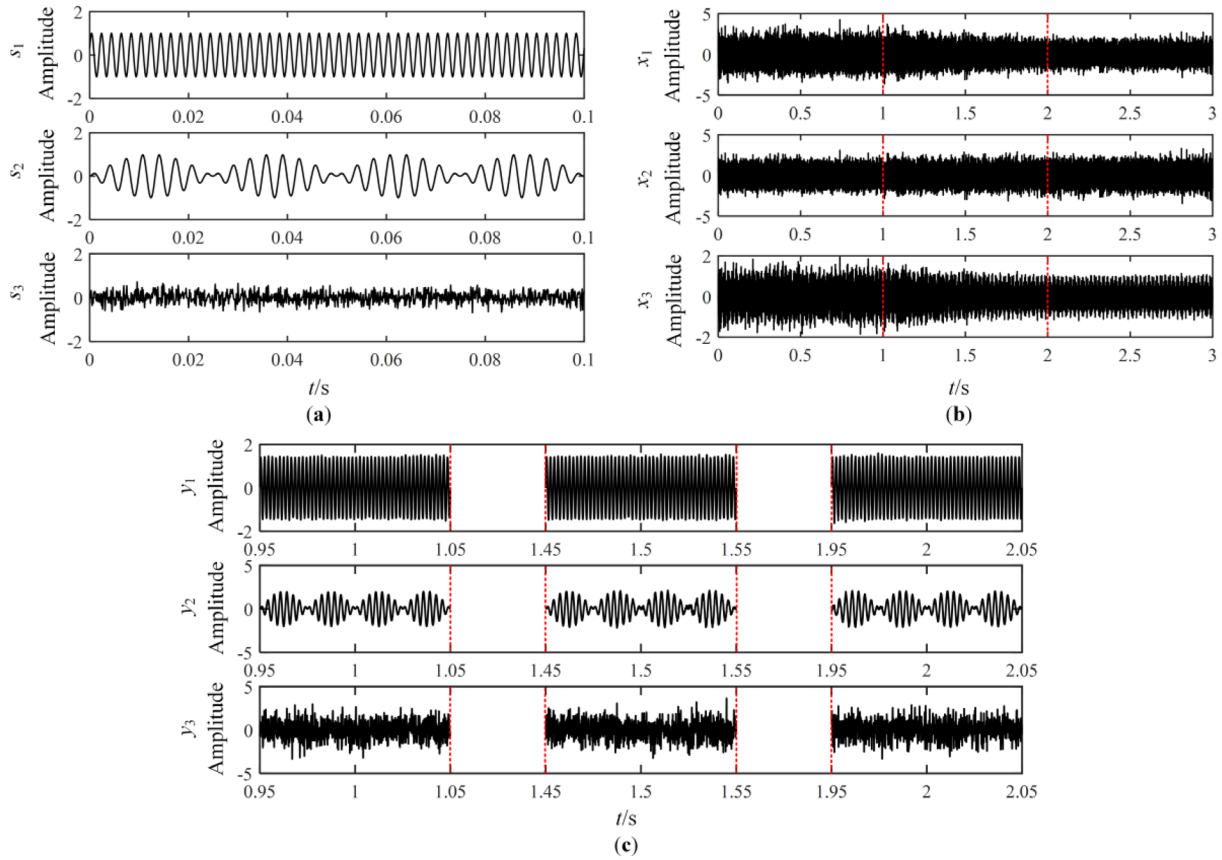

Figure 10. Separation example of the proposed method in time-varying cases. (a) Source signals; (b) mixed signals; (c) separated signals.

a small, nearly constant value. Therefore, the step size of the proposed method can be adaptively adjusted in the separation process.

Figure 7(a) shows SNR comparison with the online methods. In figure 7(a), the SNRs of AS-WO and EDS are larger than those of FS-NG and FS-EASI. We can see that the SNR of VS-SI is about 13.5 dB, while the largest SNR of the other online methods is only 11.35 dB. Compared with the contrast methods, the SNR of VS-SI increases by more than 18.94%, which indicates that the separation accuracy of VS-SI is better than that of the contrast methods.

The proposed method is also compared with some classical offline methods, using the ICALAB Ver. 3 toolbox available at [33]. The references for the offline algorithms are available in the *Help* section of the toolbox. SNR comparison between the proposed method and the offline methods is shown in figure 7(b), where the SNR of VS-SI is nearly the same as those of FPICA and SOBI, and is larger than those of JADEop and EVD2. Therefore, compared with offline methods, VS-SI still has better performance as anticipated.

4.2.2. Wide-band signals. Three swept-frequency signals are used to test the estimation performance of wide-band signals of the proposed method. The three source signals are a linear swept-frequency signal, a quadratic swept-frequency signal, and a logarithmic swept-frequency signal, and their frequency ranges are (10 Hz, 1000 Hz), (600 Hz, 1400 Hz), and (10 Hz, 1500 Hz), respectively. The sampling frequency is 4096 Hz and the sampling length is 3 s. Waveforms of the source signals and their Fourier spectra are shown in figure 8(a). In the test, the mixing matrix is randomly generated. Waveforms and Fourier spectra of the mixed signals are given in figure 8(b). Gaussian white noise is independently added to each mixed signal with SNR = 20dB. The separated signals

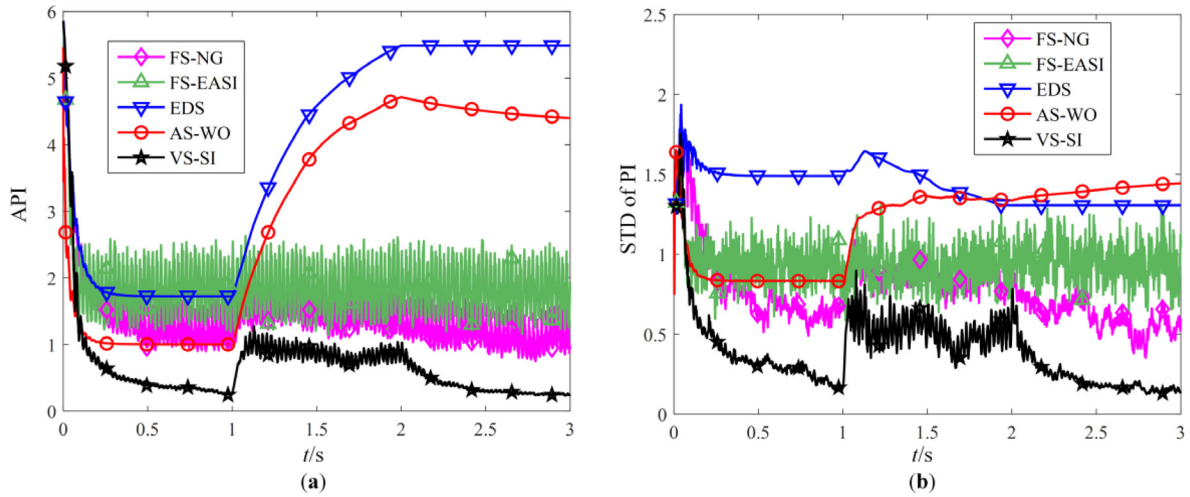

Figure 11. Performance comparison using harmonic signals in time-varying cases. (a) API; (b) STD of PI.

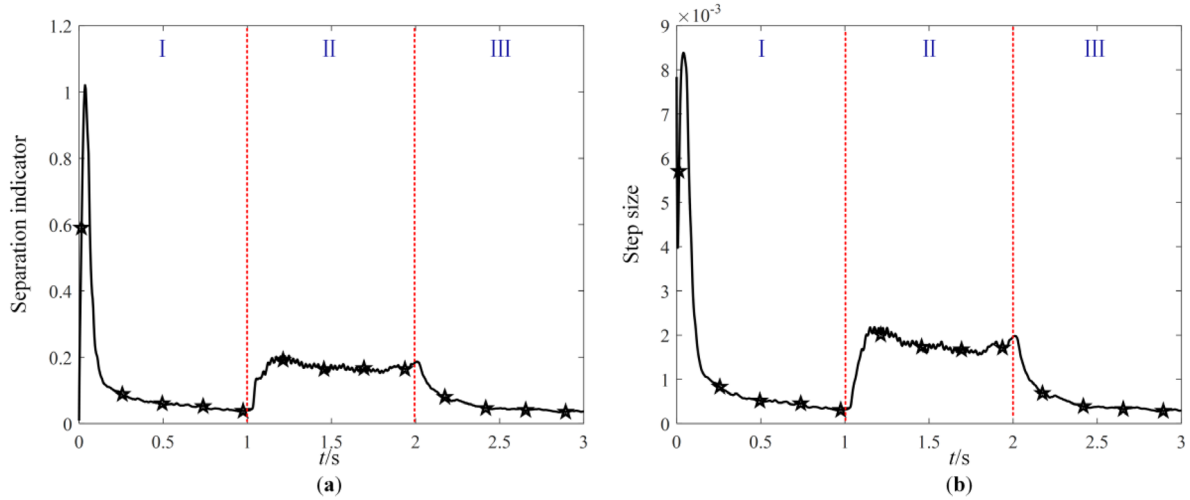

Figure 12. Variation of the SI and the step size of the proposed method in time-varying cases. (a) SI; (b) step size.

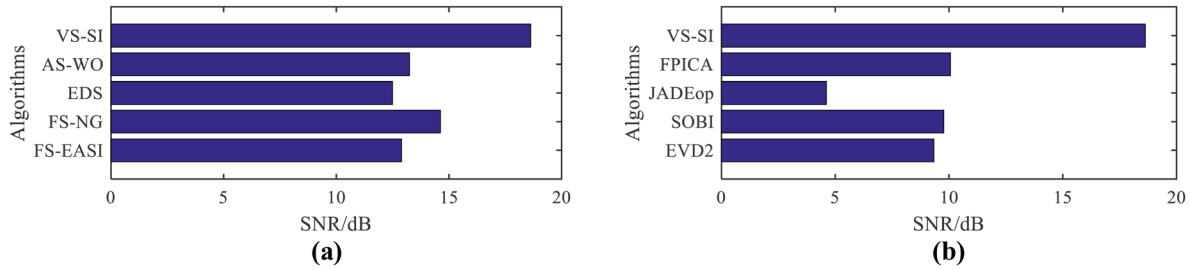

Figure 13. SNR comparison using harmonic signals. (a) Comparison with online methods; (b) comparison with offline methods.

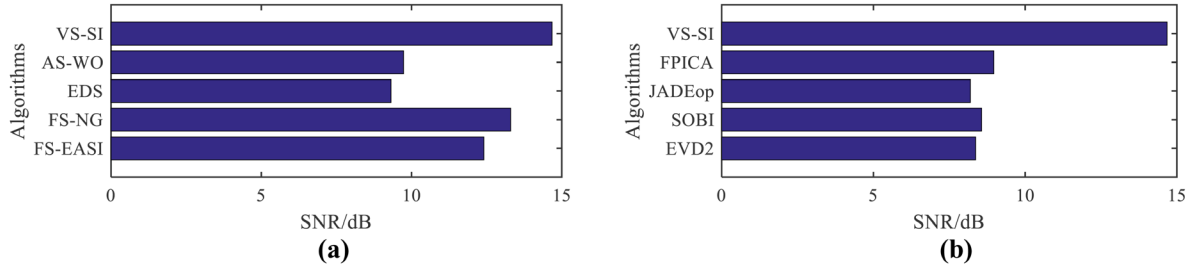

Figure 14. SNR comparison using wide-band signals. (a) Comparison with online methods; (b) comparison with offline methods.

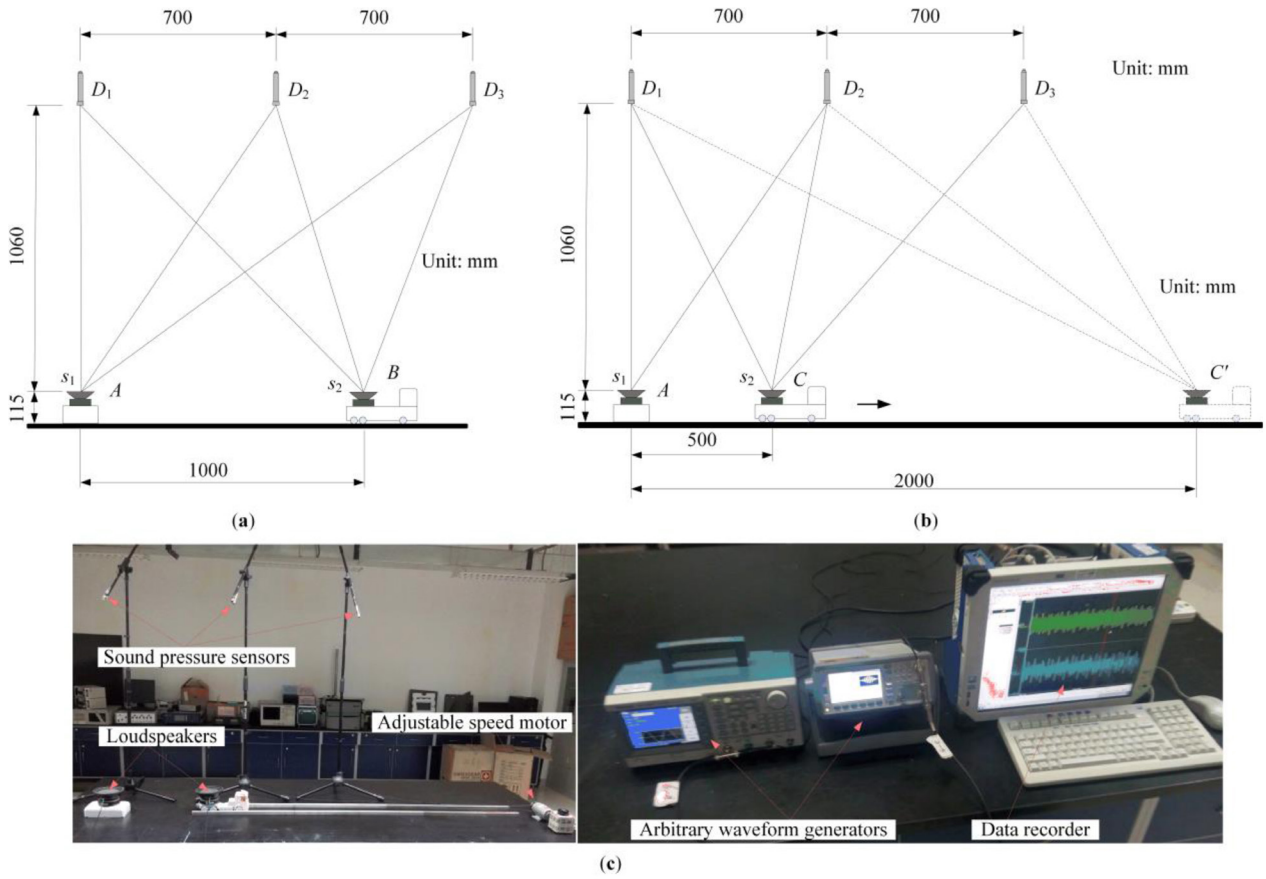

Figure 15. Structural diagram and experimental images. (a) Structural diagram in time-invariant cases; (b) structural diagram in time-varying cases; (c) images of the test bed.

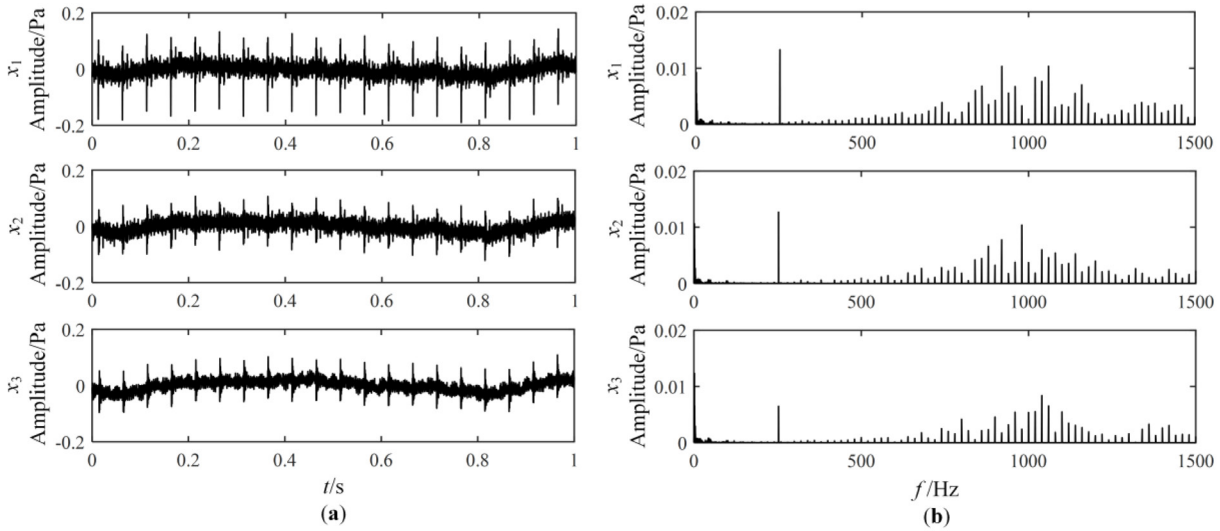

Figure 16. Mixed signals in time-invariant cases. (a) Waveforms; (b) Fourier spectra.

of the proposed method are shown in figure 8(c). Comparing figures 8(c) and (a), we can see that the source signals have been well recovered except for the amplitude and order of the separated signals.

Figure 9 shows SNR comparison with other methods. Figures 9(a) and (b) show the SNR comparison with online and offline methods, respectively. It can be seen in figure 9 that, when compared with online and offline methods, the SNR of VS-SI is the largest. Therefore, the proposed method could outperform the contrast methods while dealing with wide-band signals.

4.3. Numerical case studies in time-varying cases

4.3.1. Harmonic signals. This section explores the performance of the proposed method in time-varying cases. The source signals are

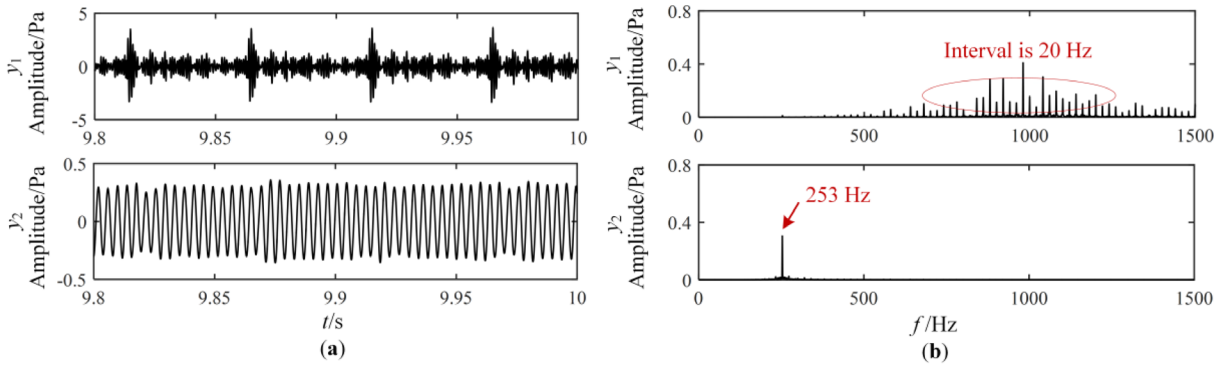

Figure 17. Separated signals in time-invariant cases. (a) Waveforms; (b) Fourier spectra.

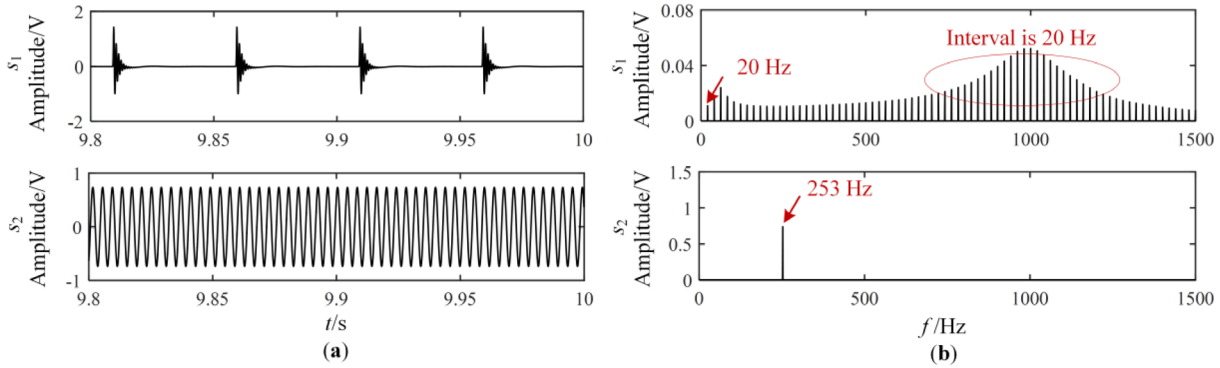

Figure 18. Source signals in time-invariant cases. (a) Waveforms; (b) Fourier spectra.

$s = \{s_{1t};\ s_{2t};\ s_{3t}\} = \{\sin(1000\pi t);\ \sin(40\pi t)\sin(600\pi t);\ \mathrm{randn}(-1, 1)\}$. The sampling frequency and the sampling length are 10 000 Hz and 3 s, respectively. Similar to the time-invariant cases, 100 Monte Carlo trials are also carried out in time-varying cases. The mixing matrix $\mathbf{A}$ is also randomly generated for each trial. The mixing matrices $\mathbf{A}$ in 0 s–1 s, 1 s–2 s and 2 s–3 s are denoted as $\mathbf{A}_1$, $\mathbf{A}_2$ and $\mathbf{A}_3$, respectively. $\mathbf{A}_1$ is randomly generated and $\mathbf{A}_3$ is defined as

$$\mathbf{A}_3 = \mathbf{A}_1 + \begin{bmatrix} -0.12 & 0.27 & -0.35 \\ -0.34 & 0.24 & 0.20 \\ 0.21 & -0.13 & -0.27 \end{bmatrix}. \qquad (26)$$

$\mathbf{A}_2$ linearly varies from $\mathbf{A}_1$ to $\mathbf{A}_3$ in 1 s–2 s. Therefore, the mixing matrix in each trial is fixed from 0 s to 1 s and from 2 s to 3 s, and the mixing matrix is time-varying from 1 s to 2 s. Gauss white noise is added to mixed signals with SNR = 20 dB.

An example of the proposed method in time-varying cases is provided in figure 10. The source signals, mixed signals and separated signals are shown in figures 10(a)–(c), respectively. From figure 10(b), the mixed signals between the two red dotted lines are time-varying. Only partial signals of the separated signals in 0.95 s–1.05 s, 1.45 s–1.55 s, and 1.95 s–2.05 s are given to clearly observe the details. Comparing figures 10(c) and (a), we can see that the separated signals are similar to the source signals and the signals in 1 s–2 s have also been well recovered.

Figure 11 shows the performance comparison in time-varying cases. Figures 11(a) and (b) present the API and

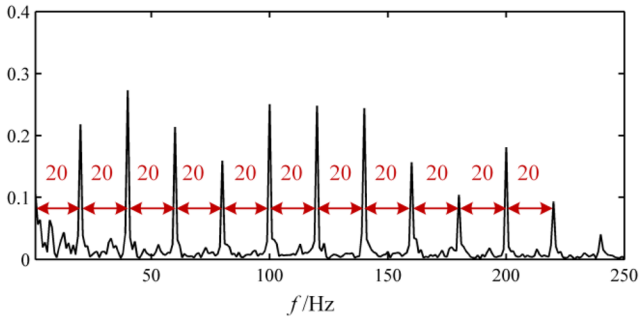

Figure 19. Envelope spectrum of y_1 separated by the proposed method.

STD of PI of the 100 Monte Carlo trials, respectively. As shown in figure 11(a), the API of the proposed method is the smallest, though it increases a little in 1 s–2 s. Since FS-NG and FS-EASI have fixed step size, their APIs are larger and have a larger degree of fluctuation. The step size of EDS at 1 s has decreased to a small value, so the API increases after 1 s. The forgetting factor in AS-WO is only suitable for station cases, and thus AS-WO seems to have worse separation performance than the proposed method in non-stationary cases. In figure 11(b), the STD of the PI of the proposed method is also the smallest, indicating that the proposed method could have better numerical robustness.

Figure 12 shows the variations of the average SI and average step size of the proposed method in time-varying cases. From this figure, the variation of both the SI and the step size can be divided into three stages: (I) At the first stage, the trends of the

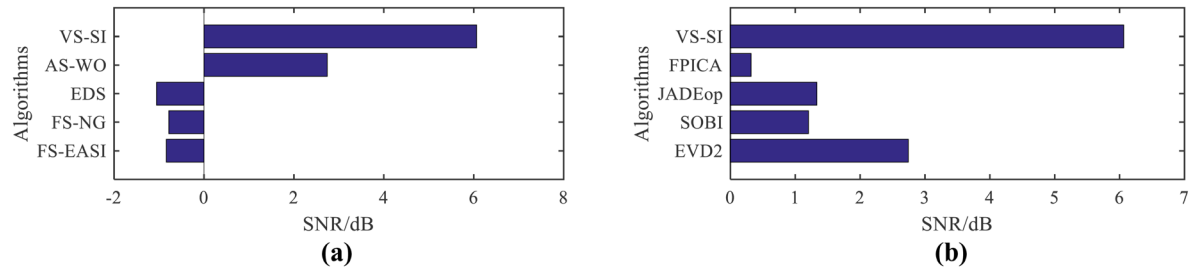

Figure 20. SNR comparison in time-invariant cases. (a) Comparison with online methods; (b) comparison with offline methods.

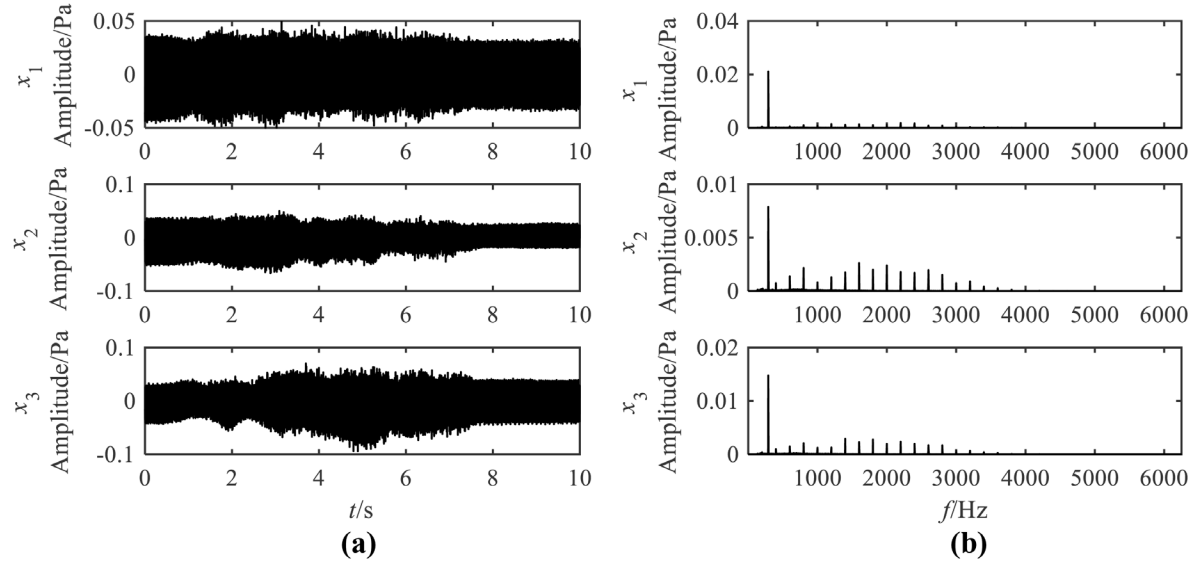

Figure 21. Mixed signals in time-varying cases. (a) Waveforms; (b) Fourier spectra.

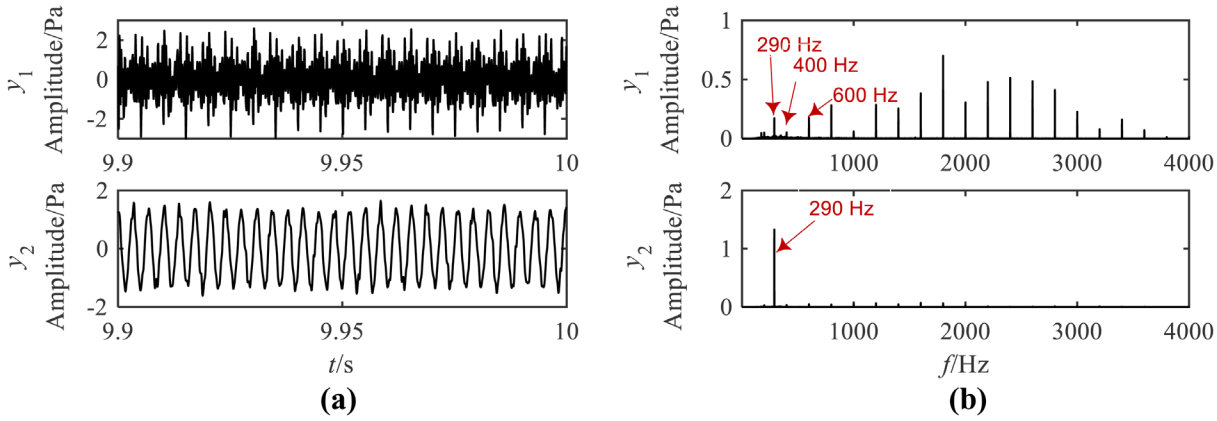

Figure 22. Separated signals in time-varying cases. (a) Waveforms; (b) Fourier spectra.

SI and the step size are similar to those of time-invariant cases. (II) At the second stage, the mixing matrix is time-varying, so the SI increases, leading to an increase in step size. (III) At the third stage, the mixing matrix is fixed, so the trends of SI and step size are similar to in the first stage. Therefore, the step size of the proposed method can be dynamically adjusted in time-varying cases.

Figure 13(a) presents SNR comparison with online methods in time-varying cases. Seen from figure 13(a), the SNRs of VS-SI, AS-WO, EDS, FS-NG and FS-EASI are 18.63 dB, 13.25 dB, 12.5 dB, 14.62 dB, and 12.9 dB, respectively. Compared with these four methods, the SNR of VS-SI increases by 5.38 dB, 6.13 dB, 4.01 dB, and 5.73 dB, respectively.

We also compare the proposed method with classical offline methods, i.e. FPICA, JADEop, SOBI and EVD2. Figure 13(b) shows SNR comparison with the classical offline methods in time-varying cases. It shows that the SNR of VS-SI increases by more than 8.57 dB compared with those of offline methods.

From figure 13, the SNRs of online methods are larger than those of offline methods, which means the separation performances of online methods are better than those of offline

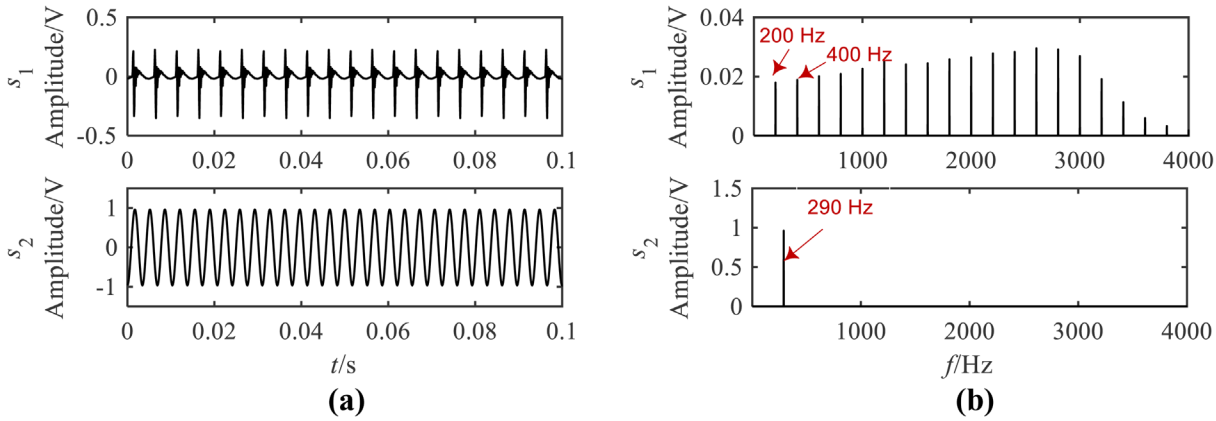

Figure 23. Source signals in time-varying cases. (a) Waveforms; (b) Fourier spectra.

methods in time-varying cases. The mixing matrix varies in time-varying cases, but a fixed mixing matrix is used to separate the source signals in offline methods, which is likely to bring about errors in the source signals. Therefore, although FPICA and SOBI can show excellent estimation performance and sometimes are even better than the proposed method in time-invariant cases, they are not suitable for time-varying cases.

4.3.2. Wide-band signals. The swept-frequency signals in section 4.2.2 are used as source signals to test the estimation performance of the proposed method for wide-band signals in time-varying cases. The sampling frequency and the sampling length are 4096 Hz and 3 s respectively. In addition, the mixing matrix is the same as in section 4.3.2, that is, it is fixed in (0 s, 1 s) and (2 s, 3 s), and varies linearly from 1 s to 2 s. In this process, Gaussian white noise is added to each mixed signal with SNR = 20 dB.

Figure 14 shows the performance comparison with online methods and classical offline methods. From figure 14, we can also see that the SNR of VS-SI is the largest compared with not only online methods but also offline methods. Compared with the largest SNRs of online and offline methods, the SNR of VS-SI increases by 1.38 dB and 5.68 dB, respectively.

5. Experimental case analysis

5.1. Experimental setup

A test bed is constructed to evaluate the performance of the proposed method. The schematic diagram and pictures of the test bed are displayed in figure 15. In the test bed, two loudspeakers placed at A and B (or C, see figures 15(a) and (b)) are used as source signals. Two arbitrary waveform generators are used to produce two different source signals that are inputs of the loudspeakers. Loudspeaker s_1 is fixed to simulate the fixed source and loudspeaker s_2 is installed in a mobile trailer model to simulate the moving source. Three sound pressure sensors, placed in D_1, D_2 and D_3, are installed to collect the mixed sound signals. A GEN2i high-speed data recorder is used to record the mixed signals.

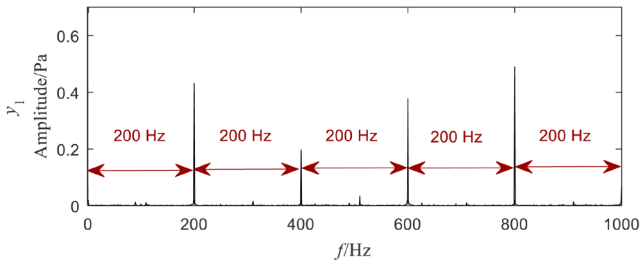

Figure 24. Envelope spectrum of y_1 separated by the proposed method.

5.2. Experimental case studies in time-invariant cases

In this case, two loudspeakers are fixed and placed at A and B, as shown in figure 15(a). The mixed signals and their Fourier spectra are shown in figure 16. The mixed signals are first processed by the proposed method. Waveforms and Fourier spectra of the separated signals are shown in figure 17, from which we can see that the two separated signals are an oscillating attenuation signal and a sinusoidal signal.

To demonstrate the performance of the proposed method, the source signals are also recorded directly from the outputs of two arbitrary waveform generators. The source signals and their Fourier spectra are shown in figure 18. From figure 18(a), the source signals are an oscillating attenuation signal with major frequency 20 Hz and a sinusoidal signal with major frequency 253 Hz. Comparing figure 17 and 18, the waveforms of the separated signals are similar to those of the source signals, and the major frequencies of the source signals have also been well recovered. It can be seen that y_1 has some difference from s_1 in the low-frequency region and the major frequency 20 Hz cannot be directly obtained from the Fourier spectrum of y_1. Therefore, the envelope spectrum of y_1 is obtained and displayed in figure 19. We can easily obtain the impact frequency 20 Hz and its higher-order harmonic.

The mixed signals are also separated by the contrast methods. The SNRs of the separated signals recovered by these methods are computed and displayed in figure 20. The SNR of VS-SI is about 6 dB, while the largest SNR of the other online and offline methods is smaller than 3 dB, which reveals that the proposed method can estimate sources more accurately than the contrast methods.

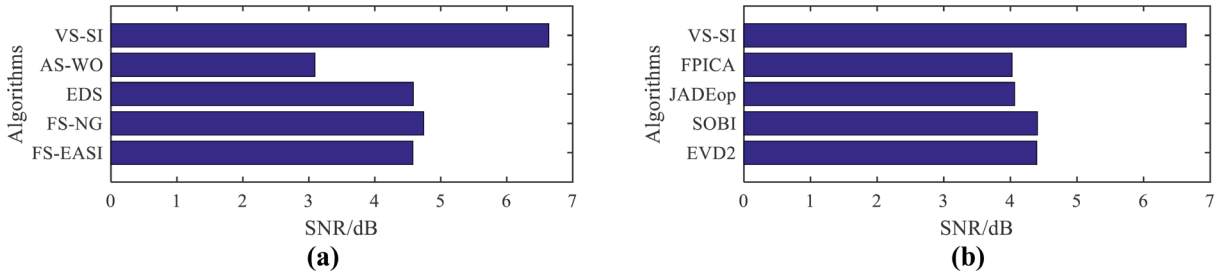

Figure 25. SNR comparison in time-varying cases. (a) Comparison with online methods; (b) comparison with offline methods.

The real mixing matrix **A** is needed to obtain the PI to analyze the convergence speed and steady-state error. However, it is difficult to obtain the real mixing matrix **A** in the experimental cases. Therefore, the convergence speed and steady-state error are not analyzed in the experimental cases and only the SNRs of the methods are given to show the high accuracy of the proposed method.

These results may show that the proposed adaptive-step-size online BSS method can recover source signals effectively from mixed signals and retain their major frequencies in time-invariant cases.

5.3. Experimental case studies in time-varying cases

In this case, two loudspeakers are placed at A and B. Loudspeaker s_2 is moved from C to C' driven by a motor, as shown in figure 15(b). Therefore, the mixing matrix is time-varying in this case. A pulse signal and a sinusoidal signal are treated as source signals. The mixed signals and their frequency spectra are shown in figure 21.

Figure 22 displays the separated signals and their spectra obtained by the proposed method. Real source signals are also recorded and illustrated in figure 23. Comparing figure 22 and 23, the waveforms of the separated signals are similar to those of the source signals, and the major frequencies of the source signals are recovered satisfactorily. Though the frequency 290 Hz still exists in the first separated signal, its amplitude has been relatively small. The envelope spectrum of y_1 (from 9 s to 10 s) is obtained and displayed in figure 24. We can easily obtain the impact frequency 200 Hz and its higher-order harmonic. These results show that the proposed method can effectively estimate source signals in time-varying cases.

The SNRs of the separated signals estimated by the proposed method and the contrast methods are also computed and displayed in figure 25. It can be seen from this figure that the SNR of the proposed method is larger than those of the contrast methods, indicating that the proposed method could outperform the contrast methods in time-varying cases.

6. Conclusion

This paper introduced an adaptive-step-size online BSS method based on EASI by adjusting the step size with the separation degree of the mixed signals. This online BSS method was able to balance the convergence speed and the steady-state error, and therefore can be used in both time-invariant and time-varying cases. In numerical case studies, the SNR of the proposed method was larger than those of other online methods for both harmonic signals and wide-band signals in time-invariant cases. In time-varying cases, the step size of the proposed method adaptively changes in accordance with the variation of mixing matrix and therefore the separation performance is better than that of the contrast online methods. Compared with offline methods, the SNR of the proposed method is not especially distinct from those of FPICA and SOBI in time-invariant cases. However, these offline methods use fixed mixing matrices to recover source signals in time-varying cases, which is likely to cause large errors in sources. Therefore, the SNR of the proposed method increases by more than 8.57 dB and 5.68 dB for harmonic signals and wide-band signals, respectively. In the experimental case studies, the proposed method tended to satisfactorily recover the waveforms of source signals and retain their major frequencies in not only time-invariant but also time-varying cases.

The proposed method can be used to recover the radiated noise signal of a moving source, such as a land or underwater vehicle, from the mixtures collected by sensors. In addition, in the proposed method, the separated signals have the problem of order indeterminacy and amplitude indeterminacy when compared with the source signals, and therefore some further research to solve these problems can be carried out in the future.

Acknowledgment

The authors appreciate the late Professor Zhengjia He sincerely for his guidance and groundwork for us. The authors would also like to thank Yingxian Zhang from the China University of Geosciences for her useful suggestions.

This work was supported by the Projects of National Natural Science Foundation of China (Grant No. 51775407 general project, Grant No. 61633001 key project), the General Project of Joint Preresearch Fund for Equipment of Ministry of Education (Grant No. 6141A02022121), the National Key Research and Development Program of China (Grant Nos. 2019YFB1705403, 2017YFC0805701), the Fundamental Research Funds for the Central Universities, and Basic Research Project of Natural Science in Shaanxi Province (Grant No. 2015JQ5183).

ORCID iDs

Wei Cheng https://orcid.org/0000-0002-2032-7815
Yanyang Zi https://orcid.org/0000-0002-3045-6514

References

[1] Oudompheng B, Nicolas B and Lamotte L 2018 Localization and contribution of underwater acoustical sources of a moving surface ship *IEEE J. Ocean. Eng.* **43** 536–46
[2] Song Y, Wen J, Yu D, Liu Y and Wen X 2014 Reduction of vibration and noise radiation of an underwater vehicle due to propeller forces using periodically layered isolators *J. Sound Vib.* **333** 3031–43
[3] Selim H, Moctezuma F P, Prieto M D, Trull J F, Martínez L R and Cojocaru C 2019 Wavelet transform applied to internal defect detection by means of laser ultrasound *Wavelet Transform and Complexity* (London: IntechOpen) (https://doi.org/10.5772/intechopen.84964)
[4] Mokhtari S A and Sabzehparvar M 2019 Application of Hilbert–Huang transform with improved ensemble empirical mode decomposition in nonlinear flight dynamic mode characteristics estimation *J. Comput. Nonlinear Dyn.* **14** 011006
[5] Wang Z, He G, Du W, Zhou J, Han X, Wang J, He H, Guo X, Wang J and Kou Y 2019 Application of parameter optimized variational mode decomposition method in fault diagnosis of gearbox *IEEE Access* **7** 44871–82
[6] Lahmiri S 2017 Comparing variational and empirical mode decomposition in forecasting day-ahead energy prices *IEEE Syst. J.* **11** 1907–10
[7] Deb S, Dandapat S and Krajewski J 2017 Analysis and classification of cold speech using variational mode decomposition *IEEE Trans. Affective Comput.* **2017** 2761750
[8] Dragomiretskiy K and Zosso D 2014 Variational mode decomposition *IEEE Trans. Signal Process.* **62** 531–44
[9] Comon P and Jutten C 2010 *Handbook of Blind Source Separation: Independent Component Analysis and Applications* (New York: Academic) (https://doi.org/10.1109/MSP.2012.2230552)
[10] Cheng W, He Z and Zhang Z 2014 A comprehensive study of vibration signals for a thin shell structure using enhanced independent component analysis and experimental validation *Trans. ASME. J. Vib. Acoust.* **136** 041011
[11] Cheng W, Lee S, Zhang Z and He Z 2012 Independent component analysis based source number estimation and its comparison for mechanical systems *J. Sound Vib.* **331** 5153–67
[12] Maazouzi F and Bahi H 2013 Type-2 Fuzzy Gaussian mixture models for singing voice classification in commercial music production *Int. J. Signal Imaging Syst. Eng.* **6** 111–8
[13] Naanaa W and Nuzillard J-M 2017 Extreme direction analysis for blind separation of nonnegative signals *Signal Process.* **130** 254–67
[14] Becker H, Albera L, Comon P, Kachenoura A and Merlet I 2017 A penalized semialgebraic deflation ICA algorithm for the efficient extraction of interictal epileptic signals *IEEE J. Biomed. Health Inform.* **21** 94–104
[15] Cheng W, Zhang Z, Lee S and He Z 2012 Source contribution evaluation of mechanical vibration signals via enhanced independent component analysis *Trans. ASME, J. Manuf. Sci. Eng.* **134** 021014
[16] Bhatnagar A, Gupta K, Pandharkar U, Manthalkar R and Jadhav N 2019 Comparative analysis of ICA, PCA-based EASI and wavelet-based unsupervised denoising for EEG signals *Computing Communication and Signal Processing* (Berlin: Springer) pp 749–59
[17] Hyvärinen A 1999 Fast and robust fixed-point algorithms for independent component analysis *IEEE Trans. Neural Netw.* **10** 626–34
[18] Rattray M, Saad D and Amari S-I 1998 Natural gradient descent for on-line learning *Phys. Rev. Lett.* **81** 5461–4
[19] Wang C, Huang H, Zhang Y and Chen Y 2019 Variable learning rate EASI-based adaptive blind source separation in situation of nonstationary source and linear time-varying systems *J. Vibroeng.* **21** 627–38
[20] Cruces-Alvarez S, Cichocki A and Castedo-Ribas L 2000 An iterative inversion approach to blind source separation *IEEE Trans. Neural Netw.* **11** 1423–37
[21] Nakajima H, Nakadai K, Hasegawa Y and Tsujino H 2010 Blind source separation with parameter-free adaptive step-size method for robot audition *IEEE Trans. Audio Speech Lang. Process.* **18** 1476–85
[22] Jafari M G, Chambers J A and Mandic D P 2004 A novel adaptive learning rate sequential blind source separation algorithm *Signal Process.* **84** 801–4
[23] Yang H H 1999 Serial updating rule for blind separation derived from the method of scoring *IEEE Trans. Signal Process.* **47** 2279–85
[24] Zhang X, Zhu X and Bao Z 2003 Grading learning for blind source separation *Sci. China* F **46** 31–44
[25] Tang X, Zhang X and Ye J 2014 Adaptive step-size natural gradient ICA algorithm with weighted orthogonalization *Circuits Syst. Signal Process.* **33** 211–21
[26] Xu P, Yuan Z, Jian W and Zhao W 2015 Variable step-size method based on a reference separation system for source separation *J. Sens.* **2015** 964098
[27] Cardoso J-F and Laheld B H 1996 Equivariant adaptive source separation *IEEE Trans. Signal Process.* **44** 3017–30
[28] Ye J, Jin H, Lou S and You K 2009 An optimized EASI algorithm *Signal Process.* **89** 333–8
[29] Chambers J, Jafari M and McLaughlin S 2004 Variable step-size EASI algorithm for sequential blind source separation *Electron. Lett.* **40** 393–4
[30] Fancourt C L and Parra L 2001 The coherence function in blind source separation of convolutive mixtures of non-stationary signals *Neural Networks for Signal Processing XI: Proc. 2001 IEEE Signal Processing Society Workshop (Piscataway)* ed C L Fancourt and L Parra (IEEE) pp 303–12
[31] von Hoff T P and Lindgren A G 2002 Adaptive step-size control in blind source separation *Neurocomputing* **49** 119–38
[32] Zhang J, Zhang Z, Cheng W, Li X, Chen B, Yang Z and He Z 2014 Kurtosis-based constrained independent component analysis and its application on source contribution quantitative estimation *IEEE Trans. Instrum. Meas.* **63** 1842–54
[33] Cichocki A, Shun-ichi A, Krzysztof S and Toshihisa T 2019 ICALAB Toolboxes (www.bsp.brain.riken.jp/ICALAB)